Effects of circular rigid boundaries and Coriolis forces on the interfacial instability in a rotating annular Hele-Shaw cell

Asmaa Abidate,[1] Said Aniss,[1] Ophélie Caballina,[2,*] and Mohamed Souhar[2]
[1]*Faculté des Sciences Aïn Chok, UFR de mécanique, BP 5366, Maarif, Casablanca, Morocco*
[2]*LEMTA-UMR CNRS 7563-ENSEM, 2 avenue de la Forêt de Haye, BP 160, Vandoeuvre-Les-Nancy 54504, France*
(Received 19 May 2006; published 20 April 2007)

We report analytical results for the development of instability of an interface between two immiscible, Newtonian fluid layers confined in a rotating annular Hele-Shaw cell. We perform a linear stability analysis and focus our study on the influence of both Coriolis force and curvature parameters on the interface instability growth rate. The results show that the Coriolis force does not alter the stability of a disturbance with a particular wave number but reduces the maximum growth rate. The results related to the role played by the confinement of the liquid layers are also shown to provide a modification of the fastest-growing mode and its corresponding linear growth rate.

DOI: 10.1103/PhysRevE.75.046307 PACS number(s): 47.15.gp, 47.20.Ma, 68.05.−n

I. INTRODUCTION

Several works have been devoted to analyze the interfacial instability in an annular rotating Hele-Shaw cell both theoretically and experimentally [1–9]. The fingering instability is driven by the density difference between the two liquids: the interface between a heavy fluid (water) and a light fluid (air) is unstable when the heavy fluid is accelerated in the direction of the light fluid; this phenomenon is called the Rayleigh-Taylor instability. This instability is also accompanied by a radial viscous flow. The linear problem which is restricted to the case of high density and high viscosity contrast was performed by Schwartz [2]. In his work, the Coriolis force is included in an *ad hoc* manner and it was shown that a circular drop is unstable both to translation and, depending on the rotation rate, to a number of fingering modes. Later on, Miranda [3] considered the case where the inner fluid is a magnetic liquid in the presence of an azimuthal external magnetic field. Using a linear stability analysis and neglecting Coriolis force, he has determined the growth rate when both centrifugal and magnetic forces are included and has shown that the magnetic forces tend to stabilize the interface. Recently, Gadêlha and Miranda [4] carried out a linear and weakly nonlinear stability analysis of interfacial instability in a rotating Hele-Shaw cell and have examined the effects of viscosity contrast, surface tension coefficient, and dimensionless gap spacing on finger competition. In this study the velocity gradients, which are related to internal friction in the fluid, are taken into account in the equilibrium condition. Following Schwartz [2], Waters and Cummings [5] have considered flow in a rotating Hele-Shaw cell taking into account Coriolis forces. The exact solution of the velocity field was determined and the value of the Eckman number corresponding to the fastest-growth rate was obtained in the limit of high density and high viscosity contrast and compared with results of Schwartz [2]. More recently, the same authors [12] have considered the interfacial instability of an initially circular fluid-fluid interface to provide insights into the tissue growth in a rotating bioreactor. They have developed a linear stability analysis where the time-dependent inertia and Coriolis terms are retained. They have addressed the case of a thin-disk reactor (Hele-Shaw cell) with a vertical axis and have provided an implicit formulation of the dispersion relation [see Eq. (3.26) in [12]]. The implicit formulation leading to the growth rate and the phase modulation of the pertubation is due to the time-dependent inertia. Waters and Cummings focused their discussion on the long-time-scale evolution and the short-time-scale evolution of the instability. Nevertheless, they do not include an inner radial confinement of the cell or take into account the viscous stresses in the Laplace equation at the interface. In this paper, we also consider an interface separating two fluids of different or comparable viscosity in a rotating Hele-Shaw cell. We thus undertake a linear stability analysis to describe the pertubation of the interface. The study aims to consider first the effect of inner and outer rigid boundaries. Second, we review the Coriolis effects when the time-dependent inertia is neglected. The results of the effect of Coriolis force on the growth rate are compared with those in [3,4] and in [12].

II. LINEAR STABILITY ANALYSIS

Consider two immiscible, incompressible Newtonian liquid layers confined in an annular Hele-Shaw cell (see Fig. 1). We denote by R_1 and R_2 the inner and outer radii of the cell, respectively, and by e its thickness. The cell is subject to a

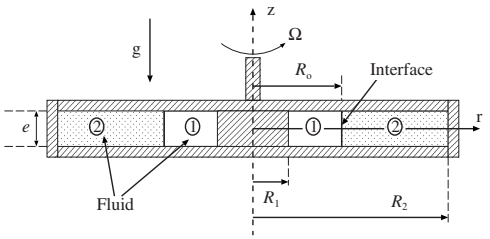

FIG. 1. Sketch of a Hele-Shaw cell with two confined liquid layers at the equilibrium. The aspect ratio $\epsilon = e/R_0, \epsilon \ll 1$.

*Electronic address: ophelie.caballina@ensem.inpl-nancy.fr

constant angular velocity $\mathbf{\Omega}=\Omega\mathbf{k}$ around its vertical symmetry axis. We assume that the equilibrium corresponds to a motionless state ($\mathbf{V_i}=0$) and a circular interface, of radii R_0, between the inner layer (fluid 1) and outer one (fluid 2). The pressure, in the rest state, is given by

$$P_i(r) = \rho_i \Omega^2 r^2/2 + C_i, \tag{1}$$

where ρ_i is the density of the fluid ($i=1,2$) and C_i is a constant. The pressure jump at the interface satisfies the Laplace-Young equation given by

$$P_1(R_0) - P_2(R_0) = \sigma/R_0. \tag{2}$$

Here, we denote by σ the surface tension between the two liquids.

Under these assumptions, the linear system describing the evolution of disturbances upon the base-state approximation is expressed in a reference frame rotating with the cell and is given by the following Navier-Stokes equations [10] including centrifugal and Coriolis forces:

$$\nabla \cdot \mathbf{v}_i = 0 \quad (i=1,2), \tag{3}$$

$$\frac{d\mathbf{v}_i}{dt} = -\frac{1}{\rho_i}\nabla p_i + \nu_i \Delta \mathbf{v}_i - \mathbf{\Omega} \wedge (\mathbf{\Omega} \wedge \mathbf{r}) - 2\mathbf{\Omega} \wedge \mathbf{v}_i, \tag{4}$$

where ν_i is the kinematics viscosity of fluid ($i=1,2$) and p_i is the hydrostatic pressure. As in the traditional Hele-Shaw flow where the aspect ratio ϵ of the cell is considered smaller than unity, a first approximation is obtained from Eqs. (3) and (4) as follows:

$$0 = \frac{1}{r}\frac{\partial}{\partial r}(r u_i) + \frac{1}{r}\frac{\partial v_i}{\partial \theta} + \frac{\partial w_i}{\partial z}, \tag{5}$$

$$0 = -\frac{\partial p_i}{\partial r} + \mu_i \frac{\partial^2 u_i}{\partial z^2} + 2\rho\Omega v_i, \tag{6}$$

$$0 = -\frac{1}{r}\frac{\partial p_i}{\partial \theta} + \mu_i \frac{\partial^2 v_i}{\partial z^2} - 2\rho\Omega u_i, \tag{7}$$

$$0 = -\frac{\partial p_i}{\partial z}. \tag{8}$$

Here, r designates the distance from the axis of rotation. Using the nonslip boundary conditions at the horizontal walls, $u_i=v_i=0$ at $z=\pm e/2$, Eqs. (5)–(8) are integrated, with respect to the variable z, to obtain the velocity field determined first in [11] and used in [5]. The vertically averaged components of velocity can be written as

$$\bar{u}_i(r,\theta) = \frac{e^2}{\mu_i}\left[M_1(\gamma_i)\frac{1}{r}\frac{\partial p_i}{\partial \theta} + M_2(\gamma_i)\frac{\partial p_i}{\partial r}\right],$$

$$\bar{v}_i(r,\theta) = \frac{e^2}{\mu_i}\left[M_2(\gamma_i)\frac{1}{r}\frac{\partial p_i}{\partial \theta} - M_1(\gamma_i)\frac{\partial p_i}{\partial r}\right], \tag{9}$$

where

$$M_1(\gamma_i) = \frac{1}{8\gamma_i^2}\left[-1 + \frac{\sin(\gamma_i)\cos(\gamma_i) + \cosh(\gamma_i)\sinh(\gamma_i)}{2\gamma_i[\cosh^2(\gamma_i) - \sin^2(\gamma_i)]}\right],$$

$$M_2(\gamma_i) = \frac{1}{8\gamma_i^2}\left[\frac{\sin(\gamma_i)\cos(\gamma_i) - \cosh(\gamma_i)\sinh(\gamma_i)}{2\gamma_i[\cosh^2(\gamma_i) - \sin^2(\gamma_i)]}\right].$$

Here, $\gamma_i = 1/(2\sqrt{E_i})$ and $E_i = \nu_i/(\Omega e^2)$ is the Eckman number representing the ratio of viscous to Coriolis forces. One can notice that the averaged velocity field obtained with this formulation including Coriolis forces differs from the classical Darcy's law used by several authors [3,4,6,9] valid for small rotation. Indeed, we verify that $M_1(\gamma_i)\to 0$ and $M_2(\gamma_i) \to -1/12$ when $E_i \to \infty$ leading to Darcy's law: $\mathbf{v}_i = (-e^2/12\mu_i)\nabla p_i$.

To investigate the dynamical evolution of the interface in a rotating Hele-Shaw cell, we describe the instantaneous interface in polar coordinates as $R=R_0+\xi(\theta,t)$, where $\xi(\theta,t)$ is an infinitesimal perturbation of the circular interface. Hereafter, we seek the solution of the linear problem in terms of normal modes as

$$[\bar{u}_i, \bar{v}_i, p_i](r,\theta) = [\tilde{u}_i(r), \tilde{v}_i(r), \tilde{p}_i(r)]e^{jn\theta},$$

with $j^2=-1$. We denote by n the azimuthal wave number, and it is an integer such as $n \geqslant 1$. Using Eqs. (9) and averaging the continuity equation with respect to the coordinate z, one obtains

$$\frac{d^2\tilde{p}_i}{dr^2} + \frac{1}{r}\frac{d\tilde{p}_i}{dr} - \frac{n^2}{r}\tilde{p}_i = 0, \tag{10}$$

and thus

$$\tilde{p}_i(r) = C_i^1 r^n + C_i^2 r^{-n}, \quad n \geqslant 1. \tag{11}$$

The four constants are determined using boundary conditions $u_1(R_1)=u_2(R_2)=0$ and the kinematics condition linearized at the interface $\partial\xi/\partial t \approx \bar{u}_i$ at $r=R$. To complete the set of equations, we must provide the dynamic boundary condition at the interface ($r=R$):

$$(P_1 + p_1) - (P_2 + p_2) + 2\left[\mu_1 \frac{\partial \bar{u}_1}{\partial r} - \mu_2 \frac{\partial \bar{u}_2}{\partial r}\right] = \sigma \nabla \cdot \mathbf{n}. \tag{12}$$

The second term on the left-hand side of Eq. (12) represents the stresses originated by normal velocity gradients. Alvarez-Lacalle *et al.* [6] have shown that this additional term turns out to be relevant because it introduces a dependence of the linear growth rate on gap spacing e and contrast viscosity A. Nevertheless, the correction affects only modes of large wave number. The curvature of the interface is written in its linearized form as

$$\nabla \cdot \mathbf{n} = -\frac{1}{R_0}\left[1 - (1-n^2)\frac{\xi(\theta,t)}{R_0}\right].$$

The total pressure is linearized as follows:

$$(P_i + p_i) = P_i(R_0) + \left.\frac{\partial P_i}{\partial r}\right|_{r=R_0} \xi(\theta,t) + p_i(R_0).$$

Finally Eq. (12) leads to the linear dimensional growth rate

$$\lambda(n) = \frac{\dot{\xi}_n}{\xi_n} = \frac{\frac{\sigma}{R_0}\epsilon^2 n[B-(n^2-1)]}{\frac{\mu_2}{1-\delta_2^{2n}}\left[\frac{1}{IM_2}+\frac{\delta_2^{2n}}{IM_2^*}\right]-\frac{\mu_1}{1-\delta_1^{2n}}\left[\frac{1}{IM_1}+\frac{\delta_1^{2n}}{IM_1^*}\right]+2\delta n\epsilon^2[\mu_1(-1+nd_1)-\mu_2(-1+nd_2)]}, \tag{13}$$

where $IM_1=M_2(\gamma_1)+jM_1(\gamma_1)$ and $IM_2=M_2(\gamma_2)+jM_1(\gamma_2)$, and IM_1^* and IM_2^* are the complex conjugate of IM_1 and IM_2, respectively. The quantities d_1 and d_2 are given by $d_1=\frac{1+\delta_1^{2n}}{1-\delta_1^{2n}}$ and $d_2=\frac{1+\delta_2^{2n}}{1-\delta_2^{2n}}$. The coefficients $\delta_1=R_1/R_0$ and $\delta_2=R_2/R_0$ represent the parameters of curvature of the inner and outer circular boundaries, respectively, and $B=(\frac{1}{\sigma})[R_0^3(\rho_1-\rho_2)\Omega^2]$ is the Bond number. The parameter δ enables to take or not into account the viscous stress in the jump equation (12) ($\delta=0$ when the viscous stress is not included and $\delta=1$ when the viscous stress is considered). Note that if we take $\delta=0$ and $\delta_1=0$, Eq. (13) can be written as

$$\lambda(n) = \frac{\frac{\sigma}{R_0}\epsilon^2 n[B-(n^2-1)]}{\frac{\mu_2}{1-\delta_2^{2n}}\left[\frac{1}{IM_2}+\frac{\delta_2^{2n}}{IM_2^*}\right]-\mu_1\frac{1}{IM_1}}, \tag{14}$$

which can be obtained from the recent paper of Waters and Cummings [12]. So our equation (13) extends their recent work by taking into account the effects of the containment and the effects of the viscous normal stresses. Whatever the considered case, one can note that the cutoff azimuthal mode number n_{cut} can be determined by Eq. (13) and $n_{cut}=\sqrt{(B+1)}$ as already shown by [4]. In the next sections, we discuss the effect of the circular rigid boundaries and that of Coriolis force on the instability.

III. EFFECT OF THE INNER AND OUTER BOUNDARIES WITHOUT CORIOLIS FORCES ($E_1\to\infty, E_2\to\infty$)

To analyze the influence of the curvatures on interface instability, we consider the case in which the Coriolis forces are neglected [$M_1(\gamma_i)\to 0$ and $M_2(\gamma_i)\to -1/12$]. In this situation, the velocity field is given by Darcy's law and the dimensionless growth rate derived from Eq. (13) is given by

$$\frac{\dot{\xi}_n}{\xi_n} \approx \bar{\lambda}(n) = \frac{n[B-(n^2-1)]}{ID+\frac{\delta n\epsilon^2}{6}[nID+A]}, \tag{15}$$

where $\bar{\lambda}(n)=[12(\mu_1+\mu_2)R_0^3/e^2\sigma]\lambda(n)$, $ID=(d_1-d_2)/2-A(d_1+d_2)/2$, and $A=(\mu_2-\mu_1)/(\mu_2+\mu_1)$ is the contrast viscosity with $-1\leqslant A\leqslant 1$. In the limit case corresponding to $d_1=1(\delta_1\to 0)$ and $d_2=-1(\delta_2\to\infty)$, we obtain the linear dimensionless growth rate obtained by Gadêlha and Miranda [see Eq. (8) in [4]] and Alvarez-Lacalle *et al.* [see Eq. (18) in [6]]. In these works, the parameters of control are B (Bond number) and A. Moreover, the addition of extra stresses introduces a dependence on the aspect ratio of the cell $\epsilon=e/R_0$. Here, one can notice that Eq. (15) is conveniently written in terms of five relevant dimensionless parameters of the problem: B, A, ϵ, δ_1, and δ_2. In our study, even if $\delta=0$, the dependence on contrast viscosity A still remains originated by the curvature parameters δ_1 and δ_2 of the inner and outer boundaries. The first information which can be extracted from the linear growth rate concerns the criterion of instability, $\lambda(n)>0$, which is similar to that of previous studies [3,4,7] and it is not affected by the parameters A, ϵ, δ_1, and δ_2. Nevertheless, the amplitude of perturbation and particularly the fastest-growing mode $n_{\max}$, defined as the integer mode n that provides the largest growth rate $\lambda_{\max}$, depend on the parameters A, ϵ, δ_1, and δ_2. This mode tends to dominate at the onset of the instability and determine the number of the fingers in the final stage [7].

Figure 2 depicts dimensionless growth rate $\bar{\lambda}(n)$ versus the wave number n with the presence of the inner boundary (b), the outer boundary (c), and both inner and outer boundaries (d). These curves are obtained for $B=200$, $A=0$, $\delta_1=0.95$, $\delta_2=1.1$, and $\epsilon=0.05$. By inspecting Fig. 2, we can see how the presence of radial walls to confine the Hele-Shaw cell modifies the linear growth rate $\bar{\lambda}(n)$. Comparing our results with those of Gadêlha and Miranda [4] [curve (a) in Fig. 2], we observe that instability is damped in the presence of boundaries. The largest growth rate $\lambda_{\max}$ decreases, and the corresponding fastest-growing mode $n_{\max}$ is weakly shifted to larger values of azimuthal wave numbers. In Fig. 3, we show, for different values of viscosity contrast A, the evolution of the growth rate as a function of the azimuthal wave number. We remark that $\lambda_{\max}$ decreases dramatically as the viscosity contrast decreases from $A=1$ ($\mu_1=0$) to

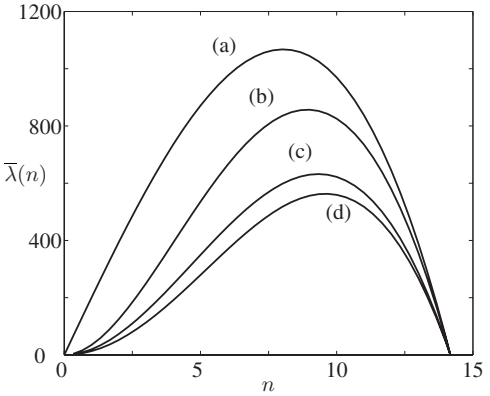

FIG. 2. The effect of boundaries on the instability. (a) $\delta_1=0$, $\delta_2\to\infty$ [4], (b) $\delta_1=0$, $\delta_2=1.1$, (c) $\delta_1=0.95$, $\delta_2\to\infty$, and (d) $\delta_1=0.95$, $\delta_2=1.1$. All data are for $B=200$, $A=0$, and $\epsilon=0.05$.

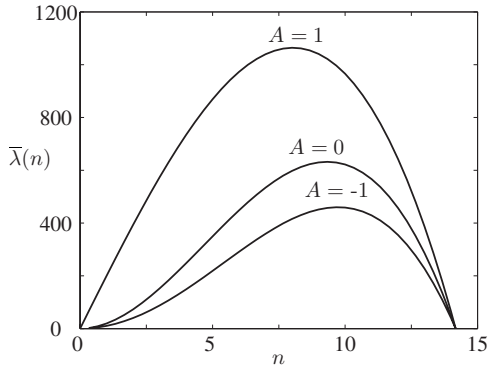

FIG. 3. The effect of contrast viscosity with the presence of the inner boundary on the instability. All data are for $B=200$, $\epsilon=0.05$, $\delta_1=0.95$, and $\delta_2\to\infty$.

$A=-1$ ($\mu_2=0$). Therefore, we can see that viscosity ratio plays a significant role even at the linear stage. Note that similar conclusions can be found from the recent work of Waters and Cummings [12] in the case $\delta_1=0$ and $\delta=0$.

IV. EFFECTS OF CORIOLIS FORCE

The previous studies dealing with the Coriolis forces on the stability of an interface in a rotating Hele-Shaw cell are those performed by Schwartz [2] and Waters and Cummings [5,12]. In the former paper, the Coriolis term is included in an *ad hoc* manner. In their first paper, Waters and Cummings have derived a model with the exact form of the Coriolis term and have concluded that the model used by Schwartz [2] can lead to appreciable errors. Nevertheless, both studies have dealt with the case of high density and high viscosity contrast (water-air for example). In their second paper, Waters and Cummings have extended their results to the general case of two viscous fluids. In the present study, the main differences are the confinement of the cell and the use of an interface boundary condition which incorporates stresses originated from normal velocity gradients. And we restrict our study to the case with no time-dependent inertia leading

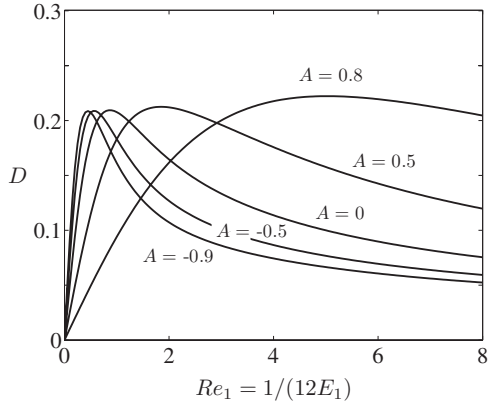

FIG. 4. Comparison of growth rate for different values of contrast viscosity and for $\rho_1/\rho_2=1000$, $\delta_1=0$, and $\delta=0$. Note that the curve $A=-1$ should produce the same results of Waters and Cummings [5].

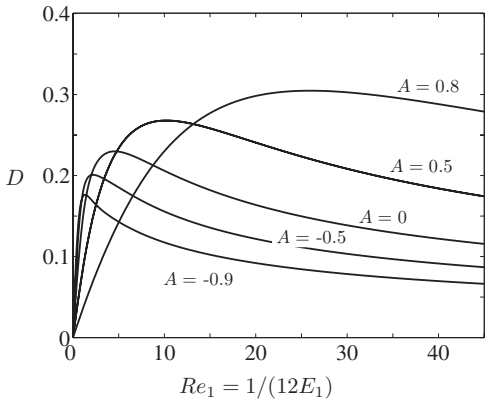

FIG. 5. Comparison of growth rate for different values of contrast viscosity and for $\rho_1/\rho_2=1.5$, $\delta_1=0$, and $\delta=0$. These results can be obtained from the recent paper of Waters and Cummings [12].

to an explicit formulation of the dispersion relation compared to [12].

In such a configuration, the linear stability analysis provides that

$$\mathrm{Re}[\lambda(n)]=\frac{\frac{n}{E_1}\left[1-\frac{n^2-1}{B}\right]\left[1-\frac{\rho_2}{\rho_1}\right]\Omega H}{H^2+G^2},$$

$$\mathrm{Im}[\lambda(n)]=\frac{\frac{n}{E_1}\left[1-\frac{n^2-1}{B}\right]\left[1-\frac{\rho_2}{\rho_1}\right]\Omega G}{H^2+G^2},$$

with

$$H=\left[\frac{1+A}{1-A}\frac{M_2(\gamma_2)d_2}{M_1^2(\gamma_2)+M_2^2(\gamma_2)}-\frac{M_2(\gamma_1)d_1}{M_1^2(\gamma_1)+M_2^2(\gamma_1)}+2\delta n\epsilon^2\left((-1+nd_1)-\frac{1+A}{1-A}(-1+nd_2)\right)\right],$$

$$G=\left[-\frac{1+A}{1-A}\frac{M_1(\gamma_2)}{M_1^2(\gamma_2)+M_2^2(\gamma_2)}+\frac{M_1(\gamma_1)}{M_1^2(\gamma_1)+M_2^2(\gamma_1)}\right].$$

We remark that in the presence of Coriolis forces, the growth rate is complex and the imaginary part corresponds to waves traveling in the azimuthal direction. In order to be as clear as possible, we consider the stability of an interface between two unbounded liquid layers ($\delta_1=0$ and $\delta_2\to\infty$). The case of high viscosity and density contrasts, $A=-1$ ($\mu_2=0$), $\rho_2=0$ and $\delta=0$, was studied in [5]. Those authors have given the variation of the dimensionless parameter $D=[1-(\rho_2/\rho_1)]H/[E_1(H^2+G^2)]$ versus Reynolds number of the inner fluid defined as $\mathrm{Re}_1=1/(12E_1)$ and shown that the growth rate is maximized for $\mathrm{Re}_1=1/(12E_1)=0.423$. Here we are interested in the configuration where the outer fluid is also viscous. In Figs. 4 and 5 we present a variation of the previously mentioned parameter D versus the inner Reynolds number Re_1 for different values of contrast viscosity and for $\rho_1/\rho_2=1000$ and $\rho_1/\rho_2=1.5$. We observe that the inner Reynolds number for which the growth rate is maximized in-

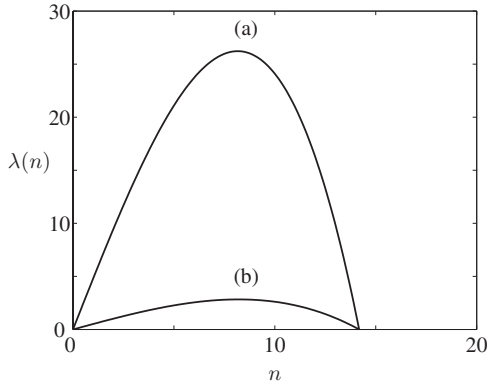

FIG. 6. Water-air interface ($\sigma=0.072$ N/m, $R_0=10$ cm, $e=2$ mm): variation of the dimensional growth rate versus n (a) without Coriolis forces [3,4] and (b) with Coriolis forces.

creases with the contrast viscosity and the values of this number are largest in the first case ($\rho_1/\rho_2=1000$) than in the second one ($\rho_1/\rho_2=1.5$). Indeed, when the viscosity of the outer fluid increases, the maximum of growth rate is obtained for fast rotations (small Eckman numbers). This maximum is obtained, as expected, for more rapid rotations near $\rho_1/\rho_2=1$ (stable equilibrium configuration).

Figure 6 shows for a water-air interface that Coriolis force is stabilizing in the sense that the maximum growth rate decreases. The physical reason for that is related to the large friction at the horizontal walls which leads to the suppression of inertial effects. Quite the same situation takes place in the case of a porous medium when Darcy's law is assumed for the resistance force.

Figure 7 shows for a water-air interface that the term including the viscous stresses [$\delta=1$ in Eq. (13)] turn out to be relevant even at the linear stage. By introducing a dependence on gap spacing e and contrast viscosity A as already shown by Alvarez-Lacalle *et al.* [6] in a linear stability analysis but not including Coriolis effects, this additional term provides a significant correction to the relation obtained by Waters and Cummings [12]. It tends to increase the growth rate and to shift its maximum to higher values. So one can note that the correction especially affects the mode of large wave numbers.

V. CONCLUSION

In this study, we have conducted a linear stability analysis of the behavior of a circular interface between two fluids confined in a rotating annular Hele-Shaw cell. This theoretical approach has provided us the linear growth rate of the perturbation for each wave number.

We have focused our analysis on both the effect of the presence of circular rigid boundaries and that of Coriolis force on the linear instability of the interface. Neglecting these two contributions in our formulation leads to previous results of Gadêlha and Miranda [4] or Alvarez-Lacalle *et al.* [6] obtained for cases of low- and high-contrast viscosity.

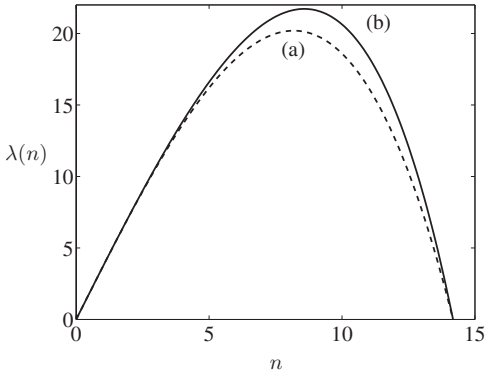

FIG. 7. Water-air interface ($\sigma=0.072$ N/m, $R_0=1$ cm, $e=1.5$ mm, $B=200$, $\delta_1=0$, $\delta_2\to\infty$): variation of the dimensional growth rate versus n in presence of Coriolis effects. (a) Dashed line: without viscous stresses obtained either by Eq. (3.26) [12] or by Eq. (13) of the present study with $\delta=0$. (b) Solid line: with Coriolis forces and viscous stresses obtained by Eq. (13) of the present study with $\delta=1$.

Including the Coriolis terms in our study provides some similar results presented by Waters and Cummings for high viscosity contrast [5] and two viscous fluids [12]. The differences with these later studies lie in the fact that we neglect the time-dependent inertia terms leading to an explicit formulation of the growth rate, and we introduce an inner confinement and include the normal velocity gradient in the Laplace equation at the interface. On the role played by the rigid boundaries studied, for the sake of reliability, without Coriolis forces, we have shown that the instability is damped in the presence of walls. Moreover, we have seen that the viscosity contrast plays a significant role even at the linear stage. This point differs from the case without radial walls, where this parameter affects the instability only when the viscous stresses are taken into account at the interface [6]. Nevertheless, this dependence on the viscosity contrast A appears whatever the configuration when the Coriolis effects are considered. To discuss the role played by the Coriolis forces, we have considered the situation where the circular rigid boundaries are missing and with no time-dependent inertia in comparison with the work of Waters and Cummings [12]. We also find that the Coriolis force tends to suppress the maximum growth rate of instability. We have shown that the inner Reynolds number, corresponding to the maximum of growth rate, increases with contrast viscosity. These results are not explicitly discussed by Waters and Cummings [12]. Finally, we outline the role played by the viscous stresses which directly affects the amplitude of the growth rate and the wave number corresponding to its maximum.

ACKNOWLEDGMENTS

The authors greatly acknowledge financial support from the Centre National de la Recherche Scientifique (CNRS) France and the Centre National pour la Recherche Scientifique et Technique (CNRST) Maroc.

[1] P. G. Saffman and G. I. Taylor, Proc. R. Soc. London, Ser. A **245**, 312 (1958).
[2] L. W. Schwartz, Phys. Fluids A **1**, 167 (1989).
[3] J. A. Miranda, Phys. Rev. E **62**, 2985 (2000).
[4] H. Gadêlha and J. A. Miranda, Phys. Rev. E **70**, 066308 (2004).
[5] S. L. Waters and L. J. Cummings, Phys. Fluids **17**, 048101 (2005).
[6] E. Alvarez-Lacalle, J. Ortin, and J. Casademunt, Phys. Fluids **16**, 908 (2004).
[7] D. P. Jackson and J. A. Miranda, Phys. Rev. E **67**, 017301 (2003).
[8] L. Carrillo, J. Soriano, and J. Ortin, Phys. Fluids **12**, 1685 (2000).
[9] L. Carrillo, F. X. Magdaleno, J. Casademunt, and J. Ortin, Phys. Rev. E **54**, 6260 (1996).
[10] H. P. Greenspan, *The Theory of Rotating Fluids* (Breukelen Press, Brookline, MA, 1990).
[11] S. Ramezani, S. Aniss, and M. Souhar, C. R. Mec. **330**, 633 (2002).
[12] S. L. Waters, L. J. Cummings, K. M. Shakesheff, and F. R. A. J. Rose, IMA J. Math. Appl. Med. Biol. **23**, 311 (2006).